Available online at www.sciencedirect.com
SCIENCE DIRECT®
Physica E 25 (2004) 47–54
PHYSICA E
www.elsevier.com/locate/physe

Size effects on the melting of nickel nanowires: a molecular dynamics study

Yu-Hua Wen[a], Zi-Zhong Zhu[a,*], Ruzeng Zhu[b], Gui-Fang Shao[c]

[a]*Department of Physics, Xiamen University, Xiamen 361005, PR China*
[b]*LNM, Institute of Mechanics, Chinese Academy of Sciences, Beijing 100080, PR China*
[c]*Department of Computer Science, Chongqing Institute of Technology, Chongqing 400050, PR China*

Received 12 April 2004; accepted 4 June 2004
Available online 2 September 2004

Abstract

The melting process of nickel nanowires are simulated by using molecular dynamics with the quantum Sutten–Chen many-body force field. The wires studied were approximately cylindrical in cross-section and periodic boundary conditions were applied along their length; the atoms were arranged initially in a face-centred cubic structure with the [0 0 1] direction parallel to the long axis of the wire. The size effects of the nanowires on the melting temperatures are investigated. We find that for the nanoscale regime, the melting temperatures of Ni nanowires are much lower than that of the bulk and are linear with the reciprocal of the diameter of the nanowire. When a nanowire is heated up above the melting temperature, the neck of the nanowire begins to arise and the diameter of neck decreases rapidly with the equilibrated running time. Finally, the breaking of nanowire arises, which leads to the formation of the spherical clusters.
© 2004 Elsevier B.V. All rights reserved.

PACS: 61.46.+w; 68.18.Jk; 87.64.Aa

Keywords: Melting; Nanowire; Molecular dynamics

1. Introduction

Materials based on nanometer-sized structures exhibit unique mechanical, electronic, optical, and magnetic properties, opening up a range of new applications [1]. As one of the most important one-dimensional (1D) nanometer materials, metal nanowires have attracted a great deal of interests in recent years, because of their great importance in fundamental low-dimensional physics as well as in technology [2–8]. The melting behavior of nanowires have exhibited dramatically different character from their bulk counterpart both

*Corresponding author: Fax: +86-592-218-9426.
E-mail address: zzhu@xmu.edu.cn (Z.-Z. Zhu).

1386-9477/$ - see front matter © 2004 Elsevier B.V. All rights reserved.
doi:10.1016/j.physe.2004.06.048

experimentally and theoretically [9–19]. As we know, for crystals the structure is an important determinant to their melting process which starts from the surface layer and propagates into the interior; the melting temperature of surface is significantly lower than that of the bulk [9,10]. Surface atoms have fewer nearest neighbors and weaker bonding which could lead to an earlier surface melting behavior [15,16]. It has been established experimentally that the melting begins preferentially at the surface in the melting process of nanoparticles and nanorods [18,19]. Qi et al. [20] reports that the melting proceeds from the surface inwards, and the mesoscale regime is characterized by the surface melting. It is therefore to be expected that the melting temperature of a nanowire decreases with the reduced diameter size, because the fraction of the atoms that resides in or near a surface increases drastically. However, the molecular dyhnamic (MD) studies for the helical multi-walled cylindrical gold nanowires by Wang et al. [21] demonstrate that the melting process starts from the interior region; the surface melting happens at relatively higher temperatures. They argue that the surface melting represents the overall melting in ultrathin metallic nanowires. Therefore, it is also important to study and/or compare the melting behaviors for different materials under different configurations.

Since metal nanowires have a number of exciting potential applications in nanoscale electronic devices, it is necessary to develop a quantitative understanding of the thermodynamic and structural properties of such metal nanowires. Computer simulation at the atomic level provides a useful tool to analyze structural, mechanical and thermodynamic properties of nanomaterials, and eventually to design materials of assigned characteristics. MD simulation, as one of the most important methods of atomistic simulations, may display the phase-space trajectories of particles through the solution of Newton's equation, thereby shedding light on how atomic level processes can lead to macroscopic phenomena, and provides a useful complement to experimental studies based on STM or AFM. MD simulations have already been employed to study the structures and properties of free-standing metal nanowires [4,9,12,14,18–21]. In the present work, we report the melting process of Ni nanowires using MD simulations, and investigate the size effect on the overall melting temperatures of the nanowire in the nanoscale regime.

2. Simulation methods

For the Ni–Ni interactions, we have used the quantum corrected Sutten–Chen (Q-SC) type many-body force field modified by Kimura et al. [22] in which the parameters were optimized to describe the lattice parameter, cohesive energy, bulk modulus, elastic constants, phonon dispersion, vacancy formation energy, and surface energy, which leads to an accurate description of many properties of metals and their alloys. With SC frame the total potential energy of the metal is taken as.

$$U_{\mathrm{tot}} = \sum_i U_i = \sum_i \varepsilon \left[\sum_{j \neq i} \frac{1}{2} V(r_{ij}) - c\sqrt{\rho_i} \right]. \quad (1)$$

Here $V(r_{ij})$ is a pair potential defined by the following equation:

$$V(r_{ij}) = \left(\frac{a}{r_{ij}} \right)^n \quad (2)$$

accounting for the repulsion between the ith and jth atomic cores. ρ_i is a local density accounting for the cohesion associated with atom i defined by

$$\rho_i = \sum_{j \neq i} \phi(r_{ij}) = \sum_{j \neq i} \left(\frac{a}{r_{ij}} \right)^m, \quad (3)$$

In Eqs. (1)–(3), r_{ij} is the distance between atoms i and j; a is a length parameter scaling all spacings (leading to dimensionless V and ρ); c is a dimensionless parameter scaling the attractive terms; ε sets the overall energy scale; n and m are integer parameters such that $n > m$. Given the exponents (n, m), c is determined by the equilibrium lattice parameter, and ε is determined by the total cohesive energy. The Q-SC potentials have already been used to study structural transitions between various phases of Ni, Cu and other face-centered-cubic (FCC) metals [23–25]. For the

Q-SC type potential of Ni, Kimura et al. give the parameters as follows: $n = 10$, $m = 5$, $\varepsilon = 7.3767E - 3$ eV, $c = 84.745$ and $a = 3.5157$ Å.

In order to simulate the melting processes of nickel nanowires and to investigate the size effects of the nanowires on the melting process, we constructed five nanowires, i.e., Ni_1.23, Ni_1.94, Ni_2.34, Ni_3.62 and Ni_4.91, representing the diameter of the nanowire ranging from 1.23 to 4.91 nm. All nanowires started with geometries constructed from a large cubic FCC single crystal of nickel using various cylindrical cutoff radii centered at a cubic interstitial site, in which the crystallographic orientations in the *X*-, *Y*-, and *Z*-axis are taken to be in the direction of [1 0 0], [0 1 0], and [0 0 1], respectively. In the *X* and *Y* directions the Ni nanowires constructed a finite number of unit cells, while in the *Z*-direction an infinite wire was obtained by applying the periodic boundary conditions. The diameter of the nanowires are in the range of 1.23–4.91 nm, which means 3.5–14 FCC unit cells, and the length of the nanowire adopt in the MD simulation is initially 17.6 nm (about 50 FCC unit cells in *Z* direction). For the simulation of the bulk system, we applied a cubic single crystal with 2048 atoms of the perfect FCC structure, and periodic boundary conditions that replicate the cube infinitely in all three spatial directions.

The molecular dynamics simulations were carried out using two styles of dynamics. The nanowires were simulated at constant temperature using NVT ensemble based on the Nose–Hoover chain dynamics [26] to have a suitable control of the temperature. The bulk systems, however, were simulated at constant temperature and constant stress based on the Parrinello–Rahman approach [27], i.e. NPT ensemble. In the MD simulations procedure, the amplitude of initial velocities of all atoms was chosen according to the Maxwell distribution, and the initial direction of the velocities were distributed randomly so that the velocity averaged over all atoms is zero and remains zero for all time steps. All the atomic trajectories were followed by integrating Newton's equation of motion for each atom with the Frog-Leap algorithm [28]. The time step in the simulation was 2.0 fs, the unit of energy was eV, and the unit of length $a_0 = 3.524$ Å which is the lattice parameter of bulk Ni at room temperature.

3. Results and discussion

In order to validate the Q-SC potential, we firstly simulate the melting process of bulk Ni and check our results with those presented in the literatures. The simulation method was as follows: firstly, the bulk Ni was relaxed at 300 K and thermalized over a period of 20,000 time steps. Doubling the duration of relaxing has no significant effect on the structure. Then the bulk Ni was subjected to heating process consisting of a series of NPT MD simulations with temperature increments of $\Delta T = 100$ K and relaxing time of 40 ps. However, for a temperature near the melting region, we used smaller temperature increment, $\Delta T = 10$ K, and the relaxation (equilibration) time still keeps 40 ps. Fig. 1 shows the temperature dependence of the average atomic potential energy (AAPE). We clearly see a sharp increase of AAPE (about 0.14 eV) at the temperature of 1700 K from the figure, which means an appearance of melting of bulk Ni. This melting temperature $T_m = 1700$ K is 28 K lower than the experimental melting temperature of 1728 K for pure Ni [29]. Our result, being very close to experimental value, shows that the Q-SC potential is suitable for investigating the melting process of metal Ni. At the same time, we also simulate the melting process of the bulk Ni at NVT ensemble. The results display that the

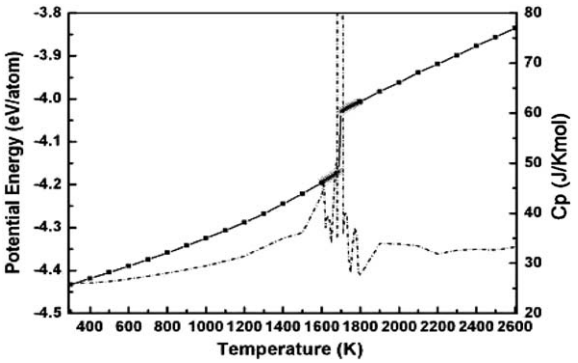

Fig. 1. The temperature dependence of the potential energy and the heat capacity C_p for bulk Ni.

melting temperature is then 3070 K, which is 1342 K higher than the experimental value. For the simulation of the melting process of the bulk, the NPT ensemble is necessary because the lattice parameters should be allowed to expand correspondingly in order to eliminate the interior stress when the temperature is increasing.

To calculate the heat capacity, we apply Eq. (3) in Ref. [20]. Fig. 1 also shows the heat capacity C_p as a function of temperature in heating process of bulk Ni. The C_p at 300 K is 25.9 J/Kmol which is very close to the experimental value of 26.1 J/Kmol for pure Ni [30]. With the increase of temperature to 1600 K, the C_p gradually increases, and then begins to fluctuate around 40 J/Kmol. An abrupt increase of C_p is found at 1700 K which means a melting transition is happening. When the temperature is higher than 1900 K, the solid state of bulk Ni is completely translated to liquid Ni, and the C_p fluctuates between 32 and 34 J/Kmol.

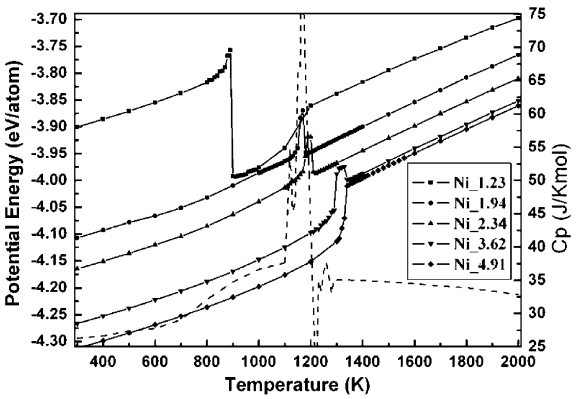

Fig. 2. The potential energies (solid lines) and heat capacity C_p (dashed line) as a function of temperature for Ni nanowires.

We now discuss our simulations on the melting of the Ni nanowires. In order to study the influence of the size of the nanowires on their melting temperatures, we have simulated the heating process of Ni nanowires with five different diameters as mentioned in the previous section. The simulation routes for Ni nanowires were similar to that of the bulk Ni except that the Ni nanowires were simulated in NVT ensemble. The temperature dependences of the AAPE of these nanowires were illustrated in Fig. 2. It can be seen that the AAPE for nanowires are higher than that of the bulk due to their surface energies, and the exceeded value of nanowire to the bulk increases as the diameter of the nanowire is reduced. The melting transition is clearly identified from the point of an abrupt increase in the potential energy, which is well defined but much broader than that of bulk. We define the overall melting temperature T_m as the maximum in the slope of potential energy as the function of temperature. Table 1 summarizes the overall melting temperatures T_m of nickel nanowires with various diameters from our simulations. Clearly, the overall melting temperatures of the nanowires are much lower than that of bulk Ni and increase when the diameters of the nanowires are increased.

The heat capacities of the nickel nanowires shown in Fig. 2 are calculated by the same formula as in Fig. 1. We plot only the Ni_2.34 nanowire as a representative. We found a broad peak in the heat capacity curve, which implies a coexistence of solid and liquid state in a rather broad temperature region below the overall melting point. The reasons may be come from the finite-size effect in the first-order phase transition [31,32]. From Fig. 2, we may classify three different regions: low, melting and high temperature ones. At

Table 1
The number of atoms in the supercell N, the diameter D and the overall melting temperature T_m of Ni nanowires, the simulated and experimental melting temperatures of bulk Ni

	Ni_1.23	Ni_1.94	Ni_2.34	Ni_3.62	Ni_4.91	Bulk Ni	Ni (exp)
N	1050	3050	6450	17,050	32,850	2048	
D(nm)	1.23	1.94	2.34	3.62	4.91		
T_m(K)	880	1160	1190	1300	1340	1700	1728

low-temperature region, the potential energy has a closely linear relation to temperature and Ni nanowires keep in the solid state. Around the melting temperature point, the potential energy begins to deviate from linearity, which means that the melting starts. The potential energy reaches its maximum at the melting point, and then decreases sharply with the further increase of temperature. The reason of an abruptly reduced AAPE is because of the breaking of the Ni nanowire and the formation of spherical clusters. At evaluated temperatures above the melting point but below 2000 K, the potential energy comes back to a linear relation with temperature which implies that the formed spherical clusters have not split into smaller ones. It should be mentioned that in our simulations the neck has not been formed in the heating of the Ni_4.91 nanowire, which can be seen from the temperature dependence of the potential energy showed in Fig. 2 where no abruptly reduced AAPE is found. The reason for this unreasonable result is simply because the length of the supercell in the Z-axis used for Ni_4.91 nanowire is not large enough. When the ratio of the length to diameter of the nanowire is too small, the neck cannot be formed.

The overall melting temperatures versus the reciprocals of the nanowire's diameters are presented in Fig. 3. A least-squares linear fit on the calculated points gives the following relation for the overall melting temperature T_m and the diameter of the nanowire D:

$$T_m = T_0 + kD^{-1} \quad (4)$$

where $T_0 = 1510\,\mathrm{K}$ is the extrapolated melting temperature of a nanowire when the diameter is infinite, i.e., the melting temperature of bulk Ni extrapolated from the curve; $k = -751.23\,\mathrm{K\,nm}$ describes the linear dependence of T_m on the reciprocal of D. The negative value of k shows that T_m increases with the increasing of the diameter. The linearly extrapolated melting temperature from Fig. 3 for Ni bulk, T_0, is significantly lower than the calculated value of 1700 K and experimental value of 1728 K of bulk Ni. The reason for the significantly lower $T_0 = 1510\,\mathrm{K}$ than the calculated value of 1700 K of bulk is not completely clear. The use of linear extrapolation in Fig. 3 may not be reasonable, i.e. the curve itself may be nonlinear at the region of large diameters (i.e. small D^{-1}), as shown by the dashed curve in Fig. 3. For the diameter region we studied, the linear relation between T_m and D^{-1} is clear. However, when the diameter of nanowire is much larger, more calculations are necessary in order to have a check on the linearity of the T_m dependence on the reciprocal of D. However, there are two similar studies that obtain the same results as in the present case. The first one is the MD simulation on the heating process of titanium nanowires by Wang et al. [18]. The extrapolated bulk melting temperature of 1542 K from the calculated melting temperature is also remarkably lower than the experimental value of 1943 K for bulk titanium. The second one is the MD simulation on the Ni nanoclusters by Qi et al. [20]. The predicted value of the melting temperature of bulk Ni is 1590 K from the T_m versus $N^{-1/3}$ for the Ni nanoclusters. Both studies got significantly lower melting temperature of bulk, when linearly extrapolated from the nanoscale studies. The predicted value of 1590 K by Qi et al. [20] from Ni nanocluster calculations are in good agreement with our result of 1510 K from Ni nanowire calculations. All these studies seem to support the argument that linear extrapolation to the bulk T_m in Fig. 3 may not be correct, i.e., the

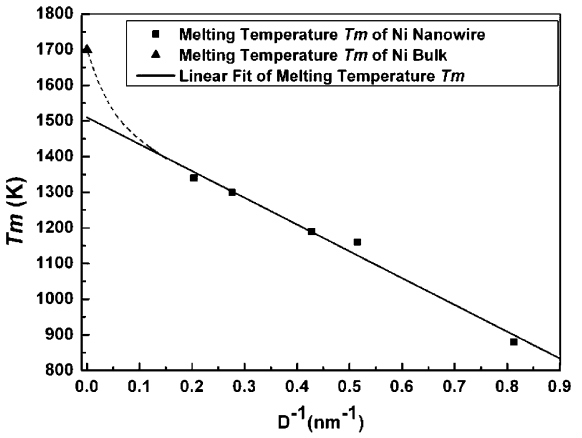

Fig. 3. The melting temperature as a function of the reciprocal of the diameter of Ni nanowire.

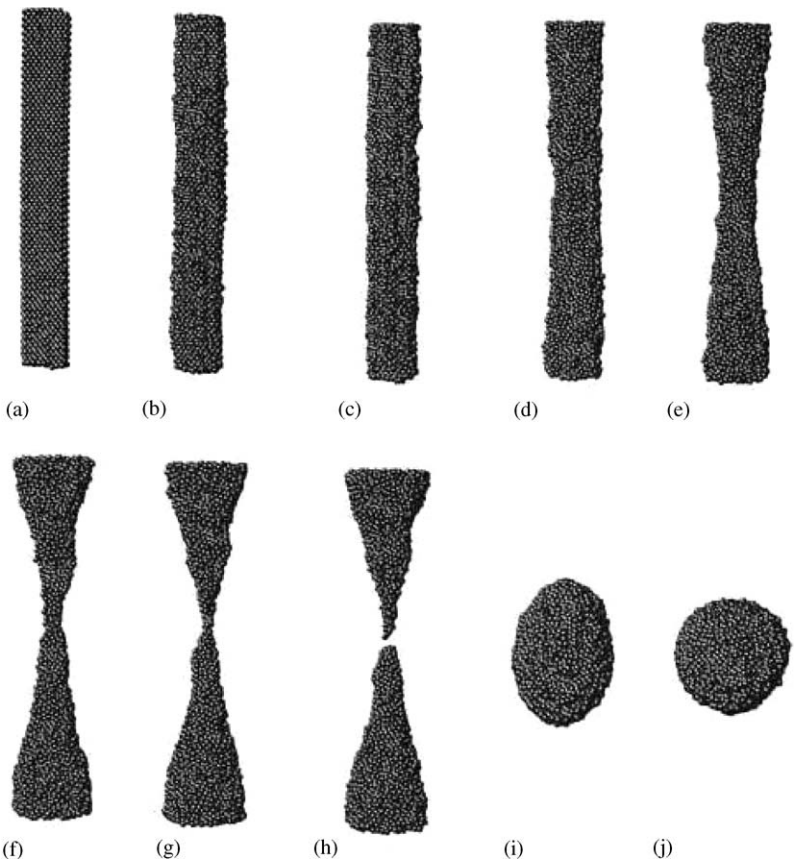

Fig. 4. (a)–(j). MD simulation snapshots of Ni_2.34 nanowire at various temperatures and times in the heating process. (a) 300 K(40 ps), (b) 1000 K(40 ps), (c) 1100 K(40 ps), (d) 1190 K(40 ps), (e) 1200 K(40 ps), (f) 1210 K(24 ps), (h) 1210 K(27.2 ps), (i) 1210 K(40 ps), (j) 1220 K(40 ps). Note that the number in the parentheses is the relaxed time of MD simulation at the corresponding temperature, that the periodic boundary condition in the axes of nanowire is applied. Formation of the clusters can be seen in Fig. 4(i) and (j).

bulk result can not be directly extrapolated from the nanoscale results. More studies are necessary in order to clarify this point.

In order to visualize the structure evolution process and to understand the melting behavior of Ni nanowires, we recorded the trajectories of atomic motions at various temperatures and times, and plotted selectively the snapshots of the melting procedure of the Ni_2.34 nanowire in Fig. 4. Fig. 4(a) shows the Ni_2.34 nanowire maintaining at the initial FCC structure. With the temperature of the system increased up to 1000 K, the surface atoms of the nanowires begin to deviate from their initial positions and a considerable disorder of some surface regions are observed during the equilibrated relaxation from Fig. 4(b). Further analysis of the structure for Ni_2.34 nanowire, by determining the local crystalline order using the common neighbor analysis [33], shows that the overall melting is accomplished at the temperature of 1190 K, which is a well-defined melting point. The neck was firstly formed in the Ni_2.34 nanowire at around 1200 K, and was relatively unstable during the relaxation. As the temperature is increased to 1210 K, disordered necks of decreasing diameters are seen as displayed in Fig. 4(f) and (g). In subsequent equilibration at the same temperature, the breaking of the nanowire can be seen in Fig. 4(h) and the further relaxation performed leads to the formation of

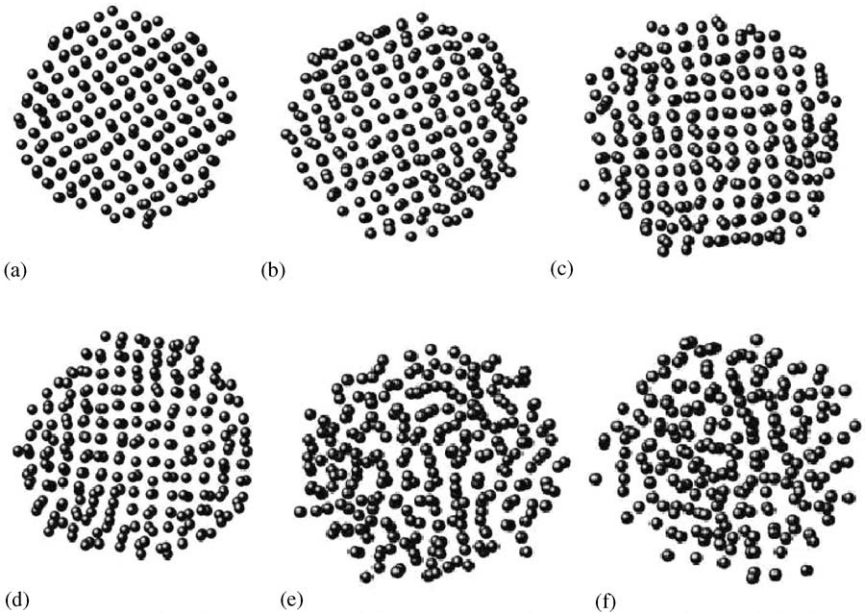

Fig. 5. (a)–(f) The X–Y sections of the same Z coordinate for Ni_2.34 nanowire at various temperatures and times in the heating process. (a) The section snapshot showing good order in the nanowire at 1000 K. (b) The section snapshot of the nanowire at 1100 K, showing that a surface melting is starting. (c)–(e) The section snapshots of the nanowire at 1130, 1160, and 1170 K, showing clearly the spread of melting process from the surface to the interior. (f) The section snapshot of the nanowire at 1190 K; the nanowire has melted completely.

clusters as shown in Fig. 4(i). The spherical clusters were finally formed by running a 40 ps at 1220 K as shown in Fig. 4(j).

In Fig. 5, we present the disorder evolution process for the nanowires in the heat-up process. Fig. 5(a)–5(f) display the atoms on the X–Y cross sections at the same Z position at 1000, 1100, 1130, 1160, 1170, and 1190 K, respectively, showing a clear picture of the spreading disorder from the surface to the interior, which means that the melting process starts from the surface layer to the interior. When the temperature reaches the melting one, T_m, the nanowire becomes entirely a disordered liquid. Remarkably, the present melting processes for the Ni nanowires are different from the case of the helical multishell gold nanowires studied by Wang et al [21], where MD simulations indicated that the melting started from the interior atoms and the surface melting happens at relatively higher temperatures. The reason for to this argument by Wang et al [21] may simply be due to the "helical multi-walled cylindrical nanowires" of Au that are used in their MD simulation.

4. Conclusions

In this paper, our simulations have demonstrated the melting process of nickel nanowires. Using MD simulations with the Q-SC force field on nickel nanowires, we show that for the nanoscale regime the overall melting temperatures of Ni nanowires are much lower than that of bulk Ni and are linear to the reciprocal of the diameter of the nanowire. When the nanowires were heated up above the melting temperature, the neck of a nanowire began to arise and the diameter of the neck decreased rapidly with the equilibrated running time. Finally, the breaking of nanowires happened leading to the formation of spherical clusters.

Acknowledgements

This work is financially supported by the National Natural Science Foundation of China (No. 10374076) and the Natural Science Foundation of Fujian Province of China (No. E0320001).

References

[1] H. Gleiter, Acta Mater. 48 (2000) 1.
[2] Y. Kondo, K.Takayanagi. Science 289 (2000) 606.
[3] B.A. Glavin, Phys. Rev. Lett. 86 (2001) 4318.
[4] B.L. Wang, S.Y. Yin, et al., Phys. Rev. Lett. 86 (2001) 2046.
[5] S. Iijima, L.C. Qin, et al., Science 296 (2002) 611.
[6] A. Bietscha, B. Michel, Appl. Phys. Lett. 80 (2002) 3346.
[7] M. Kawamura, et al., Phys. Rev. Lett. 91 (2003) 096102.
[8] N.A. Melosh, et al., Science 300 (2003) 112.
[9] O. Gulseren, F. Ercolessi, E. Tosatti, Phys. Rev. B 51 (1995) 7377.
[10] J. Hu, T.W. Odom, C.M. Lieber, Acc. Chem. Res. 32 (1999) 435.
[11] G.M. Finbow, R.M. Lynden-Bell, I.R. McDonald, Mol. Phys. 92 (1997) 705.
[12] H. Ikeda, et al., Phys. Rev. Lett. 82 (1999) 2900.
[13] G. Bilalbegovic, Solid State Commun. 115 (2000) 73.
[14] P.S. Brancio, J.P. Rino, Phys. Rev. B 62 (2000) 16950.
[15] Z. Liu, et al., Angew. Chem. Int. Ed. Engl. 39 (2000) 3107.
[16] Y. Xia, et al., Adv. Mater. 15 (2003) 353.
[17] G. Bilalbegovic, Solid State Commun. 115 (2000) 73.
[18] Z.L. Wang, et al., Phys. Rev. B 67 (2003) 193403.
[19] S. Link, et al., J. Phys. Chem. B 104 (2000) 7867.
[20] Y. Qi, T. Cagin, W.L. Johnson, W.A. Goddard, J. Chem. Phys. 115 (2001) 385.
[21] J.L. Wang, et al., Phys. Rev. B 66 (2003) 085408.
[22] Y. Kimura, Y. Qi, T. Cagin, W.A. Goddard, Unpublished.
[23] H. Ikeda, Y. Qi, T. Cagin, K. Samwer, W.L. Johnson, W.A. Goddard, Phys. Rev. Lett. 82 (1999) 2900.
[24] Y. Qi, A. Strachan, T. Cagin, W.A. Goddard III, Mater. Sci. Eng. A 309 (2001) 156.
[25] Y. Qi, Y.T. Cheng, T. Cagin, W.A. Goddard III, Phys. Rev. B 66 (2002) 085420.
[26] D.J. Evans, B.L. Holian, J. Chem. Phys. 83 (1985) 4096.
[27] M. Parrinello, A. Rahman, J. Appl. Phys. 52 (1981) 7182.
[28] M. Amini, Comput. Phys. Commun. 56 (1990) 313.
[29] C. Kittel, Introduction to Solid State Physics, Wiley, New York, USA, 1996.
[30] J.D. Cox, D.D. Wagman, V.A. Medvedev, CODATA Key Values for Thermodynamics, Hemisphere Publishing Corp., New York, USA, 1989.
[31] P. Labastie, R.L. Whetten, Phys. Rev. Lett. 65 (1990) 1567.
[32] D.J. Wales, R.S. Berry, Phys. Rev. Lett. 73 (1994) 2875.
[33] J.D. Honeycutt, H.C. Andersen, J. Phys. Chem. 91 (1987) 4950.